

Enhanced charm hadroproduction due to nonlinear corrections to the DGLAP equations*

K.J. Eskola^{a,b}, V.J. Kolhinen^{a,b,†} and R. Vogt^{c,d}

^a Department of Physics, P.O.B. 35, FIN-40014 University of Jyväskylä, Finland

^b Helsinki Institute of Physics, P.O.B. 64, FIN-00014 University of Helsinki, Finland

^c Lawrence Berkeley National Laboratory, Berkeley, CA 94720, USA

^d Physics Department, University of California, Davis, CA 95616, USA

Abstract.

We have studied the effects of nonlinear scale evolution of the parton distribution functions to charm production in pp collisions at center-of-mass energies of 5.5, 8.8 and 14 TeV. We find that the differential charm cross section can be enhanced up to a factor of 4-5 at low p_T . The enhancement is quite sensitive to the charm quark mass and the renormalization/factorization scales.

Global fits of parton distribution functions (PDFs) have been obtained by several groups, such as CTEQ [1, 2] and MRST [3, 4, 5]. These fits, based on the Dokshitzer-Gribov-Lipatov-Altarelli-Parisi (DGLAP) [6] scale evolution, fit the deep inelastic scattering (DIS) HERA data [7] on the proton structure function $F_2(x, Q^2)$ at large interaction scales $Q^2 \gtrsim 10 \text{ GeV}^2$ and momentum fractions $x \gtrsim 0.005$ very well. However, at small scales, $Q^2 \lesssim 4 \text{ GeV}^2$, and at small momentum fractions, $x \lesssim 0.005$, these fits are usually worse. In addition, the next-to-leading order (NLO) gluon distributions become very small or even negative in the small- x , small- Q^2 region. In this region, the gluon recombination terms, giving rise to nonlinear corrections to the evolution equations, become important. In a previous work [9], the first of these nonlinear terms, calculated by Gribov, Levin and Ryskin (GLR) [10] and Mueller and Qiu (MQ) [11], were included in the leading order (LO) DGLAP evolution equations of gluons and sea quarks. It was shown that the HERA DIS $F_2(x, Q^2)$ data can be reproduced well with a new PDF set‡, EHKQS, obtained in Ref. [9], employing LO-DGLAP+GLRMQ evolution.

Introducing the GLRMQ terms slows the scale evolution. At $Q^2 \lesssim 10 \text{ GeV}^2$ and $x \lesssim 0.01$, where the nonlinearities are important, this gives rise to larger gluon distributions than in the pure DGLAP case. This is shown on the left-hand side of Fig. 1, where we plot the scale evolution of the EHKQS and CTEQ61L [2] PDF sets for several

* The work of K.J.E. and V.J.K. was supported by the Academy of Finland, projects 50338, 80385 and 206024. The work of R.V. was supported in part by the Director, Office of Energy Research, Division of Nuclear Physics of the Office of High Energy and Nuclear Physics of the U. S. Department of Energy under Contract Number DE-AC03-76SF00098.

† email: vesa.kolhinen@phys.jyu.fi

‡ Available at www.urhic.phys.jyu.fi.

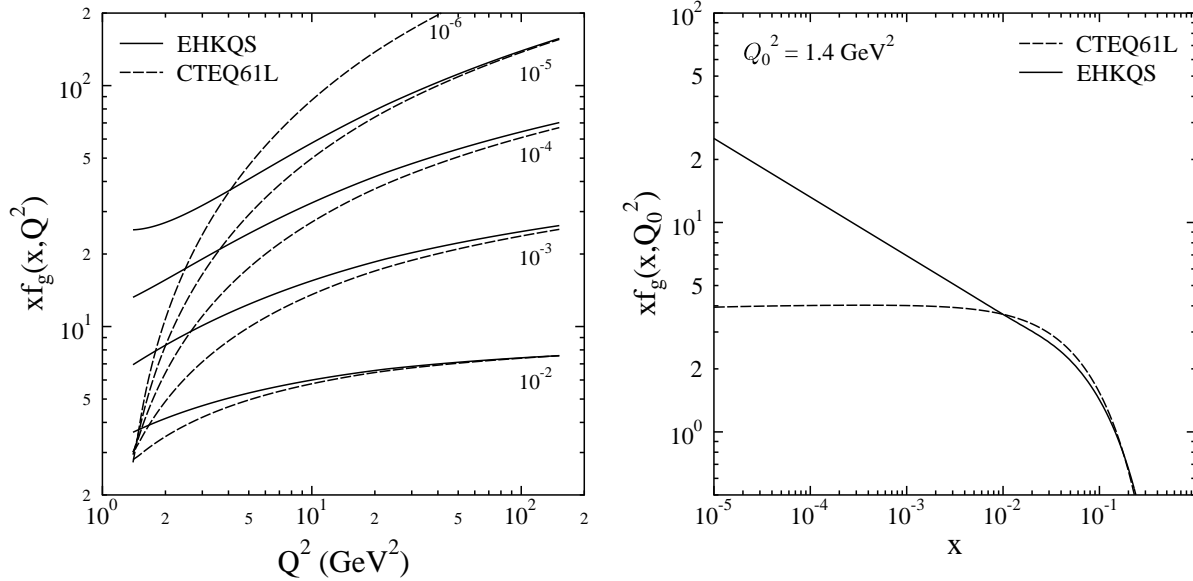


Figure 1. Left: Scale evolution of the EHKQS and CTEQ61L gluon distribution for various fixed values of x . The enhancement caused by the nonlinear terms vanishes during the evolution. **Right:** The gluon distribution as a function of x at $Q^2 = 1.4 \text{ GeV}^2$.

fixed values of x . The enhancement, large at small scales, vanishes as the nonlinear terms become negligible at larger scales. Finally, at $Q^2 \gtrsim 10 \text{ GeV}^2$, the evolution is clearly dominated by the DGLAP terms. On the right-hand side of Fig. 1 we show the gluon distributions as a function of x for $Q^2 = 1.4 \text{ GeV}^2$, the initial scale of the EHKQS set. As seen in Fig. 1, the HERA data relevant for nonlinear scale evolution suggests a factor of ~ 3 gluon enhancement at $x \sim 10^{-4}$ and $Q^2 = 1.4 \text{ GeV}^2$.

However, since the HERA F_2 data alone cannot distinguish between the linear DGLAP and nonlinear DGLAP+GLRMQ evolution, additional independent probes are needed. Here, we discuss how charm quark production in pp collisions could probe the gluon enhancement [12]. Charm production is an ideal choice since the charm mass is low and its production is dominated by gluons. Assuming factorization, inclusive differential charm cross sections at high energies can be expressed as

$$d\sigma_{pp \rightarrow c\bar{c}X}(Q^2, \sqrt{s}) = \sum_{i,j,k=q,\bar{q},g} f_i(x_1, Q^2) \otimes f_j(x_2, Q^2) \otimes d\hat{\sigma}_{ij \rightarrow c\bar{c}\{k\}}(Q^2, x_1, x_2) \quad (1)$$

where $\hat{\sigma}_{ij \rightarrow c\bar{c}\{k\}}(Q^2, x_1, x_2)$ are the perturbatively calculable partonic cross sections for charm production at scales $Q^2 \sim m_T^2 \gg \Lambda_{\text{QCD}}^2$, x_1 and x_2 are the momentum fractions of the partons involved in the hard scattering and $f_i(x, Q^2)$ are the free proton PDFs. We assume that the renormalization scale and factorization scale are equal. Only the gg and $q\bar{q}$ channels are allowed at LO, which we consider here.

We calculate the ratio of differential cross sections,

$$R(p_T, y, y_2) \equiv \frac{d^3\sigma(\text{EHKQS})/(dp_T dy dy_2)}{d^3\sigma(\text{CTEQ61L})/(dp_T dy dy_2)}, \quad (2)$$

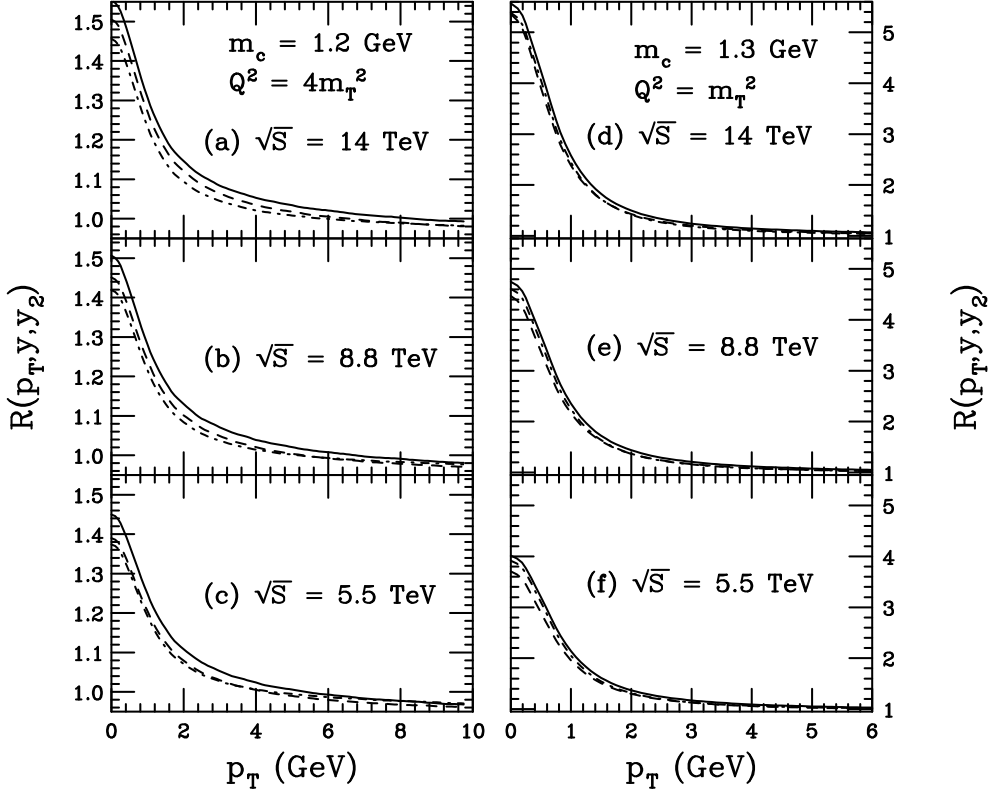


Figure 2. The ratio of differential charm cross section, $R(p_T, y, y_2)$, for fixed y and y_2 as a function of charm quark p_T at $\sqrt{s} = 14$ TeV (top) 8.8 TeV (middle) and 5.5 TeV (bottom) in pp collision. The rapidities are $y = y_2 = 0$ (solid), $y = 2, y_2 = 0$ (dashed) and $y = y_2 = 2$ (dot-dashed).

where p_T is the charm quark transverse momentum and y and y_2 are the rapidities of the charm quark and the antiquark. The results for the enhancement are plotted in Fig. 2 as a function of p_T for fixed y and y_2 . The center-of-mass energy \sqrt{s} is varied from 14 TeV (top) to 8.8 TeV (middle) and 5.5 TeV (bottom). Obviously, the largest enhancement is obtained at the largest \sqrt{s} where the x values are smallest. Different charm masses and scales are used, $m_c = 1.2$ GeV and $Q^2 = 4m_T^2$ on the left-hand side and $m_c = 1.3$ GeV, $Q^2 = m_T^2$ on the right-hand side [8]. Both of these scale choices lie within the applicability region of the PDFs. The rapidities are $y = y_2 = 0$ (solid), $y = 2, y_2 = 0$ (dashed) and $y = y_2 = 2$ (dot-dashed). For the highest energy, 14 TeV, the maximum \sqrt{s} at the LHC, the enhancement at $p_T \sim 0$ is a factor of ~ 5 for $m_c = 1.3$ GeV and ~ 1.5 for $m_c = 1.2$ GeV. We repeated the calculations for larger masses, up to $m_c = 1.8$ GeV for both $Q^2 = m_T^2$ and $Q^2 = 4m_T^2$. We found smaller enhancements, ~ 2 and ~ 1.25 at $p_T \sim 0$, respectively. Clearly, the charm enhancement can be substantial, but it is very sensitive to the choice of mass and scale. It also vanishes rapidly with p_T .

Integrating over the rapidities does not change the result much. The maximum enhancement for the rapidity-integrated ratios at small p_T at $\sqrt{s} = 14$ TeV is still ~ 4.5 for $m_c = 1.2$ GeV, $Q^2 = 4m_T^2$ and ~ 1.3 for $m_c = 1.3$ GeV, $Q^2 = m_T^2$ [9]. The ratio

of the cross sections integrated over p_T and y_2 is rather flat as a function of y , but is reduced to factors of 1.2 and 1.8 for the two low mass cases studied.

Since the DGLAP gluon distributions are already well constrained by the HERA data, they cannot absorb additional large effects. Therefore we can conclude that, if this small- p_T enhancement in the charm cross section relative to the DGLAP-based result is observed in the future experiments e.g. at the LHC, it is a signal of nonlinear effects on the PDF evolution.

As discussed in Ref. [9], the EHKQS PDFs were obtained in the region where the nonlinear terms do not dominate the scale evolution. However, at the smallest x and Q^2 of the HERA data [7] one is already close to the gluon saturation region, where all orders of nonlinearities become important [13]. Therefore these PDFs, and consequently also the charm enhancement, should be considered as upper limits. Furthermore, a full NLO DGLAP+GLR/MQ analysis would be needed for computing the charm hadroproduction enhancement consistently to NLO.

In a follow-up work [14], we show that more than half of the charm enhancement survives hadronization to D -mesons. We also show that in the most optimistic case the enhancement can be observed in the D^0 p_T spectrum in the ALICE detector at the LHC.

- [1] J. Pumplin *et al.*, JHEP **0207** (2002) 012 [arXiv:hep-ph/0201195].
- [2] D. Stump *et al.*, arXiv:hep-ph/0303013.
- [3] A. D. Martin, R. G. Roberts, W. J. Stirling and R. S. Thorne, Eur. Phys. J. C **23** (2002) 73 [arXiv:hep-ph/0110215].
- [4] A. D. Martin, R. G. Roberts, W. J. Stirling and R. S. Thorne, Phys. Lett. B **531** (2002) 216 [arXiv:hep-ph/0201127].
- [5] A. D. Martin, R. G. Roberts, W. J. Stirling and R. S. Thorne, arXiv:hep-ph/0308087.
- [6] Y. L. Dokshitzer, Sov. Phys. JETP **46** (1977) 641 [Zh. Eksp. Teor. Fiz. **73** (1977) 1216]; V. N. Gribov and L. N. Lipatov, Yad. Fiz. **15** (1972) 781, 1218 [Sov. J. Nucl. Phys. **15** (1972) 438, 675]; G. Altarelli and G. Parisi, Nucl. Phys. B **126** (1977) 298.
- [7] C. Adloff *et al.* [H1 Collaboration], Eur. Phys. J. C **21** (2001) 33 [arXiv:hep-ex/0012053].
- [8] R. Vogt [Hard Probe Collaboration], Int. J. Mod. Phys. E **12** (2003) 211 [arXiv:hep-ph/0111271].
- [9] K. J. Eskola, H. Honkanen, V. J. Kolhinen, J. w. Qiu and C. A. Salgado, Nucl. Phys. B **660** (2003) 211 [arXiv:hep-ph/0211239].
- [10] L. V. Gribov, E. M. Levin and M. G. Ryskin, Nucl. Phys. B **188** (1981) 555; L. V. Gribov, E. M. Levin and M. G. Ryskin, Phys. Rept. **100** (1983) 1.
- [11] A. H. Mueller and J. w. Qiu, Nucl. Phys. B **268** (1986) 427.
- [12] K. J. Eskola, V. J. Kolhinen and R. Vogt, Phys. Lett. B **582** (2004) 157 [arXiv:hep-ph/0310111].
- [13] K. J. Eskola, H. Honkanen, V. J. Kolhinen, J. w. Qiu and C. A. Salgado, arXiv:hep-ph/0302185.
- [14] A. Dainese, R. Vogt, M. Bondila, K. J. Eskola, V. J. Kolhinen, arXiv:hep-ph/0403098.